ISBN: 978-3-95450-184-7 doi:10.18429/JACoW-IPAC2018-THPMF085

BEAM DYNAMICS SIMULATION OF THE SOLENOID SEXTUPOLE ERROR IN THE LCLS-II INJECTOR*

J. Qiang†, LBNL, Berkeley, USA
S. D. Anderson, D. Dowell, P. J. Emma, J. Schmerge, M. Woodley, F. Zhou, SLAC, Menlo Park, USA

Abstract

The LCLS-II injector is a high brightness, high-repetition rate RF injector that consists of a 186 MHz VHF photoelectron gun, a focusing solenoid, a buncher cavity, another focusing solenoid, and a superconducting accelerating cryomodule to boost the electron beam energy to final 100 MeV. The solenoids provide transverse focusing and emittance compensation for the electron beam. However, in reality, the solenoid is not perfect due to manufacturing errors. Especially, the sextupole error in the solenoid field, which can cause significant beam emittance growth. In this paper, we report on the beam dynamics study of the effects of sextupole errors in the current LCLS-II injector.

INTRODUCTION

The LCLS-II is a 4th-generation high-repetition rate (1 MHz) Free Electron Laser (FEL) based x-ray light source to be built at the SLAC National Accelerator Laboratory that will deliver photons of energy between 200 eV and 5 keV [1, 2]. It consists of a high repetition rate photoinjector to generate and accelerate the electron beam to 100 MeV, a laser heater (LH) to suppress microbunching instability, three sections of superconducting linacs to accelerate the beam to 4 GeV, a long bypass transport line, and a magnetic kicker to spread the electron beam to a soft x-ray transport beam line and to a hard x-ray transport beam line.

The high repetition rate photoinjector consists of a VHF gun that accelerates the electron beam to 750 keV kinetic energy, a 1.3 GHz buncher cavity, and a 1.3 GHz superconduting boosting cavity that accelerates the beam to 100 MeV. There are two solenoids used in the injector: one after the VHF gun and one after the buncher cavity to provide transverse focusing for emittance compensation and focusing into the boosting cavity. Figure 1 shows the rms beam size evolution inside the LCLS-II injector with 100 pC and 300 pC beam charges. It is seen that in both cases, the beam is well focused and matched through the injector. The 300 pC beam has a larger transverse beam size than the 100 pC beam. The rms size attains a maximum about 5 and 6 mms at a location around 0.3 m downstream of the photocathode (located at 0). The fast rise of the rms size at the beginning is due to the strong space-charge defocusing effects.

In design, these two solenoids are identical and both have azimuthal symmetry. There is no sextupole error in this ideal situation. However, in practice, the solenoid is not perfect and the sextupole field errors are observed in the measurement of the solenoid. These sextupole field errors could cause beam emittance growth in the injector. In this paper, we studied the effects of the sextupole field errors in three groups of measurements on beam emittance growth using self-consistent macroparticle beam dynamics simulations.

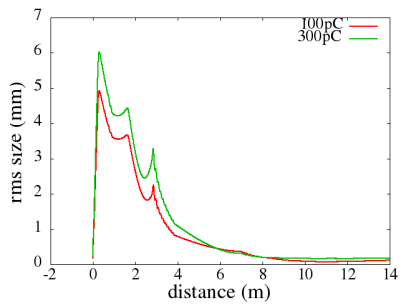

Figure 1: Root Mean Square (rms) sizes evolution through the injector for 100 pC (red) and 300 pC (green) charge beams.

COMPUTATIONAL SETUP

In this study, we have used a parallel beam dynamics simulation code IMPACT-T [3], which is apart of the IMPACT code suite [4, 5]. The IMPACT-T code is a fully three-dimensional program to track relativistic charged particles taking into account space charge forces, short-range longitudinal and transverse wakefields, coherent synchrotron radiation (CSR) wakefield in accelerators. It has a comprehensive set of beamline elements, and furthermore allows arbitrary overlap of their fields, which gives the IMPACT-T a capability to model both the standing wave structure and traveling wave structure. It includes mean-field space-charge solvers based on an integrated Green function to efficiently and accurately treat beams with large aspect ratio, and a shifted Green function to efficiently treat image charge effects of a cathode.

Before the detailed beam dynamics simulation, we simulated a cold zero emittance 750 keV electron beam transporting through a sextupole magnet without space-charge effects and compared with an analytical model. Here, the normalized normalized emittance ϵ_n increase from the analytical model is given as [6]:

$$\epsilon_n = \frac{\sqrt{3}}{2}\sigma_x^3 \frac{e}{mc} L B_{sext} \quad (1)$$

where σ_x is the electron beam rms size, m is the electron rest mass, c is the speed of light in vacuum, L is the effective length of the sextupole magnet and B_{sext} is the field

* Work supported by the U.S. Department of Energy under Contract Nos. DE-AC02-05CH11231 and DE-AC02-76-SF00515.
† jqiang@lbl.gov

ISBN: 978-3-95450-184-7 doi:10.18429/JACoW-IPAC2018-THPMF085

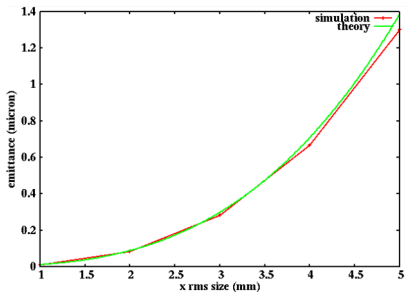

Figure 2: Normalized emittance increase as a function of rms beam size from the simulation (red) and analytical model (green).

amplitude of the magnet. Figure 2 shows the electron beam emittance increase through a 0.1 m long, 0.218 (T/m/m) sextupole magnet as a function of the beam rms size from the simulation and the analytical model. The simulation results and the analytical predictions agree with each very well. The emittance increases quickly with respect to the rms beam size. For a beam with 5 mm rms size through the sextupole, the emittance increase is beyond 1 mm-mrad.

Next we carried out detailed simulations including the measured sextupole error amplitude and phase distribution along the solenoid and the 3D space-charge effects through the injector. Here, in order to simulate the longitudinal variation of the sextupole amplitude and phase, the measured data was read into the program and interpolated to the macroparticle longitudinal location at every time step. Then, the macroparticle transverse coordinates are rotated into a frame according to the measured phase value. The horizontal and vertical sextupole magnetic fields are calculated as a regular sextupole magnet and then rotated back to the laboratory frame for macroparticle momentum advancing. In the simulation, we have used 1 million macropaticles and $64 \times 64 \times 64$ computational grid points.

SIMULATION RESULTS

Figure 3 shows the measured sextupole error amplitude and phase distribution along the longitudinal distance inside a vacuum chamber for ± 10 A and 5 A current in the solenoid. There are two peaks of the sextupole error with the major peak located around the location of maximum beam rms size. Figure 4 shows the horizontal normalized rms emittance evolution along the injector without and with the above sextupole errors in the simulations for 100 pC and 300 pC charges. The sextupole errors cause large emittance growth through the injector. For the 100 pC charge, there are a factor of 2 increase of the final emittance with 5 A current in the solenoid and a factor of 6 increase of emittance with 10 A current. For the 300 pC charge, there are a factor 4 increase of emittance with 5 A current in the solenoid and a factor of 10 increase of final emittance with 10 A current. The large emittance growth due to the above sextupole error in the solenoid is not acceptable. Improvement to the solenoid was done to reduce the sextupole error.

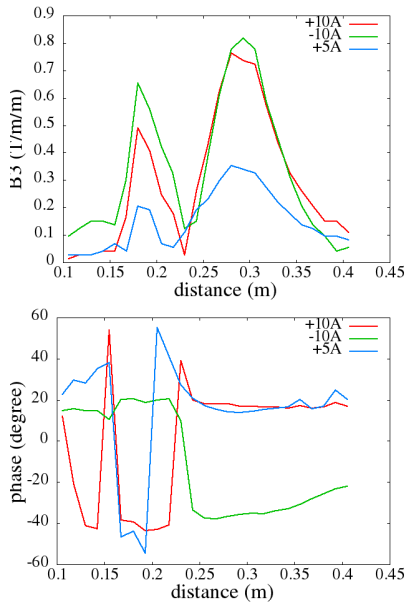

Figure 3: Sextupole error amplitude (top) and phase (bottom) as a function of distance in a solenoid with +10 A (red), −10 A (green), and 5 (blue) A current.

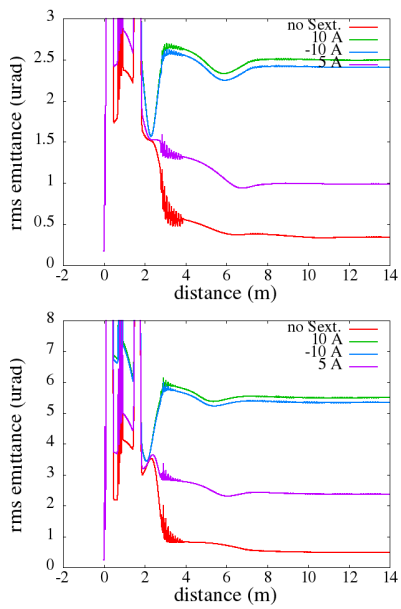

Figure 4: Projected emittance evolution without (red) and with 10 A (green), with −10 A (blue), and with 5 A current sextupole errors for 100 pC and 300 pC charges.

Figure 5 shows the sextupole field error amplitude and phase as a function of distance from a new measurement with 10 A current. Figure 6 shows the normalized horizontal rms emittance evolution without, with the above nominal measured sextupole error, and with 0.5× and 0.3× the nominal error for both 100 pC and 300 pC charges. It is seen that the final emittance growth is significantly reduced using the new measured sextupole error. For the 100 pC charge, the final emittance growth is reduced to 20% for the nominal

ISBN: 978-3-95450-184-7 doi:10.18429/JACoW-IPAC2018-THPMF085

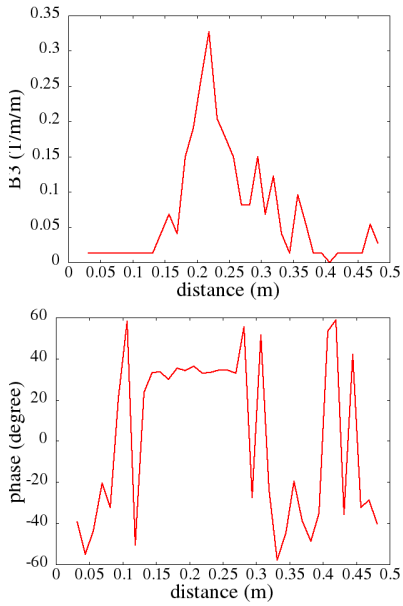

Figure 5: Sextupole error amplitude (top) and phase (bottom) as a function of distance in a new solenoid measurement.

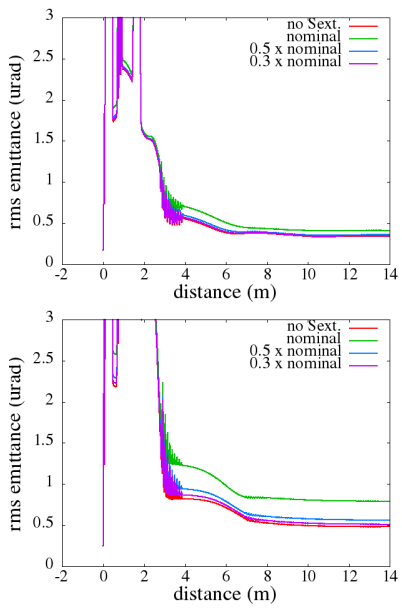

Figure 6: Projected emittance evolution without (red) and with the new sextupole error measurements for 100 pC (top) and 300 pC (bottom) charges.

error, and 5% and 2% for the 0.5× and 0.3× the nominal cases. For the 300 pC charge, the final emittance growth is reduced to 65% for the nominal error, and 17% and 6% for the 0.5× and 0.3× the nominal error. Instead of linear dependency on the sextupole field amplitude suggested in Eq. 1, the final emittance at the exit of the injector shows stronger dependency on the sextupole error amplitude in the beam dynamics simulations.

Further improvement to the solenoid manufacture and measurement results in even smaller sextupole errors in solenoid one and two. Figure 7 shows the sextupole error amplitude along the longitudinal distance for solenoid one and two. The sextupole errors in both solenoids have been

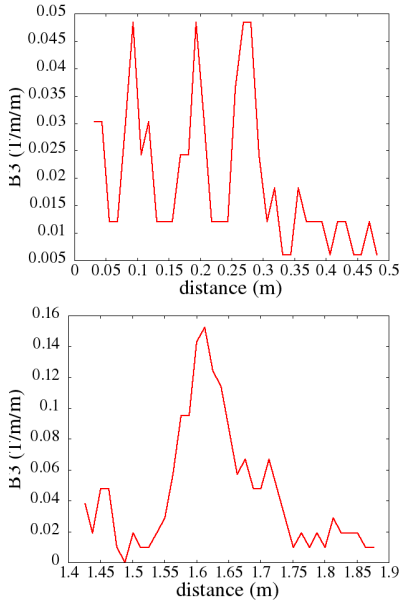

Figure 7: Sextupole error amplitude in solenoid one (top) and solenoid two (bottom) as a function of distance in a further improved measurements.

reduced. Figure 8 shows the normalized emittance evolution without and with sextupole errors for the 100 pC and 300 pC cases. With those reduced sextupole errors, the final emittance growths for both the 100 pC and 300 pC charges are below 1%.

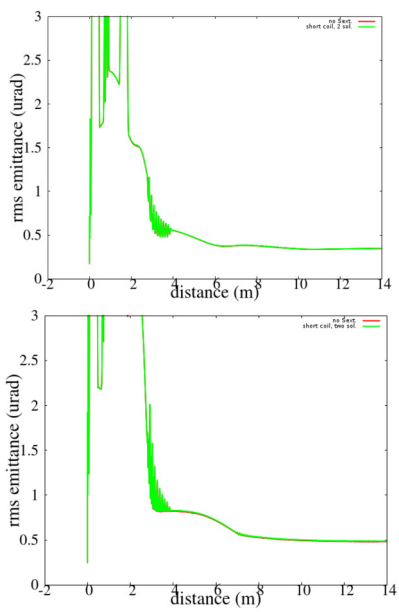

Figure 8: Projected emittance evolution without (red) and with the further improved sextupole error measurements (green) for 100 pC (top) and 300 pC (bottom) charges.

ISBN: 978-3-95450-184-7 doi:10.18429/JACoW-IPAC2018-THPMF085

ACKNOWLEDGMENT

This research used computer resources at the National Energy Research Scientific Computing Center.

REFERENCES

[1] P. Emma et al., in Proceedings of FEL14, p.743 (2014).

[2] T. O. Raubenheimer, in Proceedings of IPAC2015, p. 2434, Richmod, VA, USA (2015).

[3] J. Qiang et al., PRST-AB 9, 044204 (2006).

[4] J. Qiang et al., J. of Comp. Phys., 163, 434 (2000).

[5] J. Qiang et al., PRST-AB 12, 100702 (2009).

[6] D.H. Dowell, "Correcting emittance growth due to stray sextupole fields", SLAC-R-1091.